JOURNAL OF MATERIALS SCIENCE **39** (2004) 3079– 3083

Preparation, sintering, and microstructures of strontium barium bismuth tantalate layered perovskite ceramics

CHUNG-HSIN LU*, JIA-HAU BAI, HUNG CHEN
Electronic and Electro-Optical Ceramics Laboratory, Department of Chemical Engineering, National Taiwan University, Taipei, Taiwan, Republic of China
E-mail: chlu@ccms.ntu.edu.tw

The solid solutions of Ba-doped $SrBi_2Ta_2O_9$ layered perovskite ceramic powders have been successfully prepared via a two-step process using $BiTaO_4$ as a precursor. The lattice constants of the solid solutions monotonically increase with increasing barium-ion content. The sinterability of $(Sr_{1-x}Ba_x)Bi_2Ta_2O_9$ powders is significantly improved by increasing the barium-ion content. When the specimens with high barium-ion contents are sintered at 1100°C, they thermally decompose to form rod-like grains and the matrix expands, leading to a lower density. The addition of barium ions to $SrBi_2Ta_2O_9$ also results in significant variation in the morphology of the sintered specimens and the occurrence of *c*-axis preferred orientation which is ascribed to the anisotropic growth of plate-like grains. The precise control of the barium-ion content as well as the sintering conditions is critical for obtaining densified barium-ion doped $SrBi_2Ta_2O_9$ ceramics with a pure, layered perovskite structure.

1. Introduction

Ferroelectric materials are being intensively investigated because of their potential application to low-voltage and high-speed ferroelectric random access memories (FeRAM). Among the ferroelectric materials, the layered-structure perovskites called Aurivillius compounds [1, 2] have attracted great attention and are regarded as the prime candidate materials for FeRAM. Aurivillius compounds have a general chemical formula of $(Bi_2O_2)^{2+}(A_{x-1}B_xO_{3x+1})^{2-}$, where A and B indicate the ions with low and high valence inserting in the structures, while x is the number of octahedral structured ABO_3 in the perovskite crystals between $(Bi_2O_2)^{2+}$ layers [3]. The thin-film preparation and ferroelectric properties of Aurivillius compounds with $x = 2$ and 4, such as $SrBi_2Ta_2O_9$, $SrBi_2Nb_2O_9$, $PbBi_2Ta_2O_9$, $BaBi_2Ta_2O_9$ and $SrBi_4Ta_4O_{15}$ have been extensively investigated [4–12]. The processes for synthesizing $SrBi_2Ta_2O_9$-based thin films on Si-based substrates have been widely examined [13–16]. These studies have revealed that the layer-structured perovskites exhibit the characteristics of low leakage current, low operating voltage, stable imprinted characteristics, and high polarization retention up to 10^9–10^{12} switching cycles.

To further improve the properties of $SrBi_2Ta_2O_9$, various $SrBi_2Ta_2O_9$-based solid solutions have been studied [17–19]. $(Sr_{1-x}Ba_x)Bi_2Ta_2O_9$ thin films synthesized via a metalorganic decomposition method have shown that the grain sizes as well as the roughness of the prepared thin films increase with the added amounts of barium ions [18]. Raising the temperature can markedly enhance the remnant polarization of the specimens. Although the formation and characteristics of $(Sr_{1-x}Ba_x)Bi_2Ta_2O_9$ thin films have been studied, the sintering and microstructures of $(Sr_{1-x}Ba_x)Bi_2Ta_2O_9$ ceramics have not been studied in detail. The sintering density, stoichiometry, and preferred orientation of the raw materials have influence on the deposition rate, phase composition, and homogeneity of the obtained thin films [20, 21]. Therefore, a comprehension of the properties of the bulk ceramics is important. In this study, $(Sr_{1-x}Ba_x)Bi_2Ta_2O_9$ ceramics were synthesized using a new precursor-$BaTiO_4$. The effects of chemical composition and sintering conditions on the formation of layer-structured perovskite and the thermal stability of sintered $(Sr_{1-x}Ba_x)Bi_2Ta_2O_9$ ceramics were examined. The relations between the doping amounts of barium ions and microstructures as well as crystal orientation were also investigated.

2. Experimental

$(Sr_{1-x}Ba_x)Bi_2Ta_2O_9$ powders were fabricated via a two-step process. The starting materials, Bi_2O_3 and Ta_2O_5, were used to synthesize $BiTaO_4$, i.e., the precursor of (Sr,Ba)$Bi_2Ta_2O_9$. Both powders were weighed in accordance with the stoichiometric composition of $BiTaO_4$ and mixed by ball milling with ethanol for

* Author to whom all correspondence should be addressed.

48 h, using zirconia balls in a polyethylene jar. After the milling process, the slurry was dried in a rotary evaporator under reduced pressure. The dried mixture was heated in air and quenched at 900°C in order to form pure $BiTaO_4$ powder. In the quenching experiment, the heated samples were pulled out from the furnace and cooled in air when the set temperature reached. After pure $BiTaO_4$ powder was obtained, $SrCO_3$ and $BaCO_3$ were blended with $BiTaO_4$ by ball milling according to the stoichiometric composition of $(Sr_{1-x}Ba_x)Bi_2Ta_2O_9$ with x ranging from zero to one. The formed mixtures were quenched at 900°C without soaking to obtain the designed solidsolutions. The later quenching process was the same as the above one. In order to analyze the sintering behavior of $(Sr_{1-x}Ba_x)$ $Bi_2Ta_2O_9$, the obtained powders were pressed uniaxially into disks under 196 MPa. The disks were sintered at 1000, 1050, and 1100°C for 2 h. At the end of the sintering processes, the heated samples were naturally cooled in the furnace without further heating. The densities of the sintered disks were measured after the sintering process. X-ray diffraction (XRD) analysis using Cu K_α radiation was utilized for identifying the resultant compounds and determining the crystal lattice constants. A scanning electron microscope (SEM) was employed to observe the microstructures of the sintered specimens.

3. Results and discussion

3.1. Preparation and formation of $(Sr_{1-x}Ba_x)Bi_2Ta_2O_9$

The XRD patterns and corresponding miller indexes of $(Sr_{1-x}Ba_x)Bi_2Ta_2O_9$(SBBT) quenched at 900°C are illustrated in Fig. 1. This figure reveals that pure layered-perovskite phases are successfully synthesized by the new two-stage synthesis using $BaTaO_4$ as precursors. It is found that the Ba-doped specimens have the similar structure as that of pure $SrBi_2Ta_2O_9$, and the diffraction peaks slightly shift to the direction of low diffraction angle when the value of x is increased. These results indicate that barium ions completely replace strontium ions in the A-sites of $SrBi_2Ta_2O_9$, and the solid solutions of $(Sr_{1-x}Ba_x)Bi_2Ta_2O_9$ are formed. The lattice constants were calculated based on all diffraction peaks using a least square method. The variation of the lattice constants along a, b, and c axes as a function of x in $(Sr_{1-x}Ba_x)Bi_2Ta_2O_9$ are illustrated in Fig. 2. The lattice parameters increase nearly linearly with a rise in the value of x. Since the ionic radius of Ba^{2+}(0.134 nm) is larger than that of Sr^{2+} (0.113 nm), when barium ions replace strontium ions, the orthorhombic crystal structures begin to expand. It is also noted that when barium ions are doped in $SrBi_2Ta_2O_9$, the expansion in c-axis is greater than those in a and b axes.

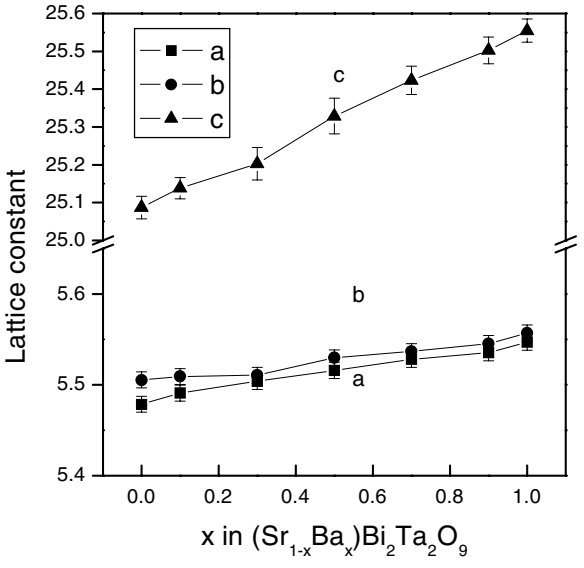

Figure 2 Lattice parameter along a, b, and c axes of $(Sr_{1-x}Ba_x)Bi_2Ta_2O_9$.

3.2. Sintering and decomposition of $(Sr_{1-x}Ba_x)Bi_2Ta_2O_9$

The obtained 900°C-quenched materials were pressed and sintered at 1000, 1050, and 1100°C for 2 h. The influence of the contents of barium ions in the sintering behavior of $(Sr_{1-x}Ba_x)Bi_2Ta_2O_9$ is shown in Fig. 3.

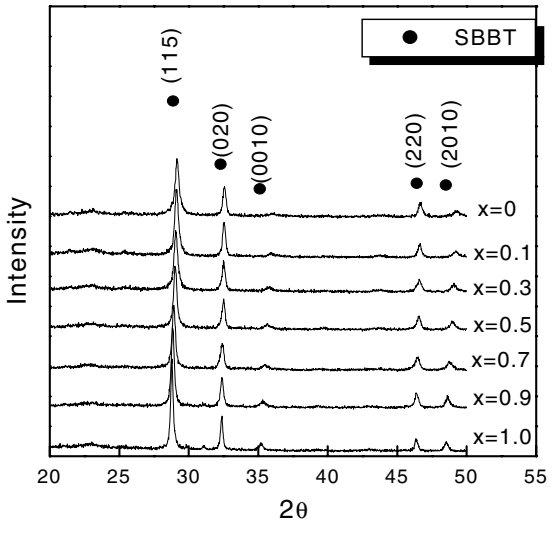

Figure 1 X-ray diffraction patterns of $(Sr_{1-x}Ba_x)Bi_2Ta_2O_9$ quenched at 900°C.

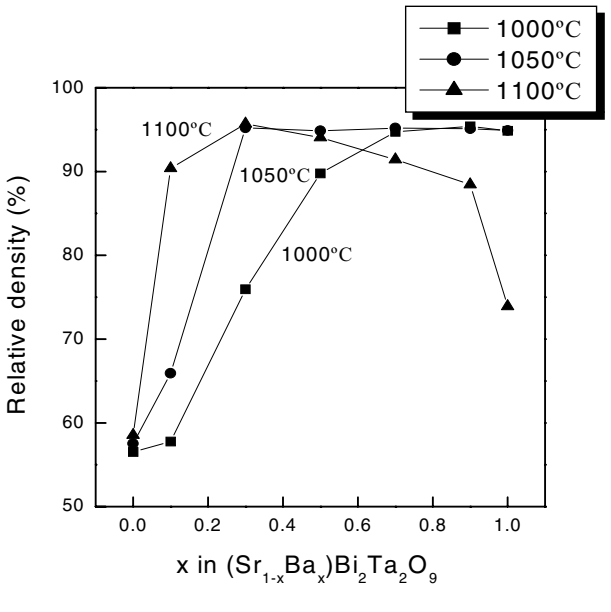

Figure 3 Relative density of $(Sr_{1-x}Ba_x)Bi_2Ta_2O_9$ sintered at 1000, 1050, and 1100°C for 2 h.

Pure $SrBi_2Ta_2O_9$ is hardly sintered at elevated temperatures. Even when the sintering temperature is raised up to 1100°C, the relative density of the heated specimen is only 58.5%. However, when the barium-ion doped specimens are sintered at 1000°C, the sinterability is effectively enhanced. The density of the specimens increases monotonously with the doping amounts of barium ions. As for the 1050°C-sintered specimens, its relative density increases to around 95.1% when the value of x reaches 0.3 ($(Sr_{0.7}Ba_{0.3})Bi_2Ta_2O_9$). On the other hand, when the specimens are sintered at 1100°C, their sintering behavior varies. At $x = 0.5$ the relative density of the specimen is around 94.2%. However, at $x > 0.5$, the density of the specimens greatly reduces with a rise in the doping amounts of barium ions. When all strontium ions are substituted by barium ions, the relative density of the specimen ($BaBi_2Ta_2O_9$) drops to 73.9%. The above results clearly demonstrate that doping barium ions into $SrBi_2Ta_2O_9$ improves the sintering properties of the specimens. However, for 1100°C-sintered specimens, high doping contents of barium ions lead to a decrease in the density, suggesting the probable decomposition of these specimens.

The surfaces of the pellets of $(Sr_{1-x}Ba_x)Bi_2Ta_2O_9$ (SBBT) were examined via XRD, and the results for the specimens sintered at 1000, 1050, and 1100°C are illustrated in Fig. 4, Figs 4–6, respectively. For all specimens sintered at 1000°C (see Fig. 4) and 1050°C (see Fig. 5), only the diffraction patterns corresponding to the structure of the layered perovskite (SBBT) are detected and these patterns are well indexed, verifying that no other phases coexist in the specimens. Nevertheless, when the sintering temperature is raised to 1100°C, various phases are formed on the surface of the specimens. At $x \leqq 0.5$, only the diffraction patterns of the layered perovskite are observed. However, a small amount of Bi_2O_3 is formed at $x = 0.7$, implying that this specimen starts to decompose. At $x = 0.9$, the amount of Bi_2O_3 increases with a corresponding decrease in the amount of the layered perovskite. When x reaches 1.0, all of the layered perovskite is completely decomposed, leaving $BaTa_2O_6$ and $Ba_5Ta_4O_{15}$ as the residual compounds.

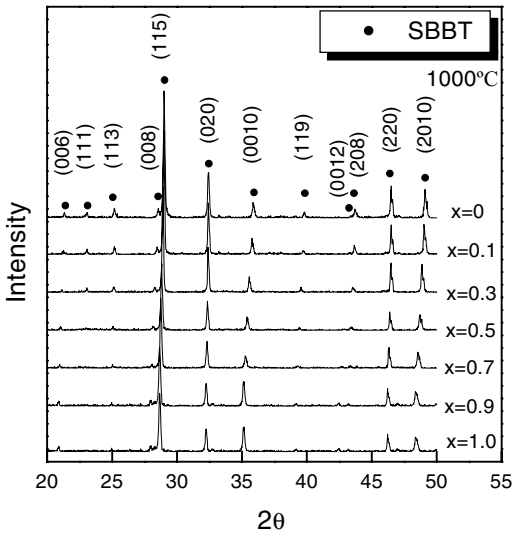

Figure 4 X-ray diffraction patterns of $(Sr_{1-x}Ba_x)Bi_2Ta_2O_9$ sintered at 1000°C for 2 h.

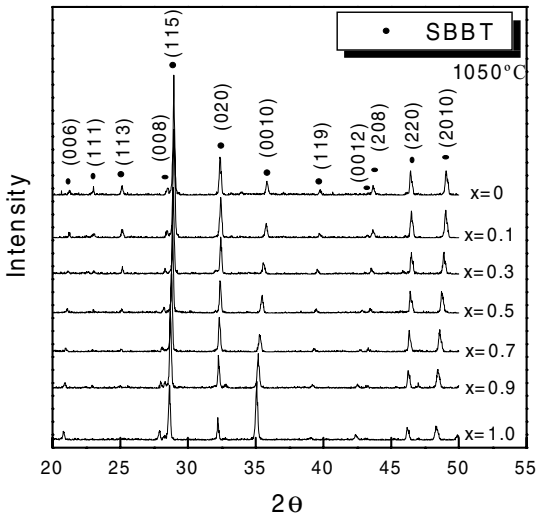

Figure 5 X-ray diffraction patterns of $(Sr_{1-x}Ba_x)Bi_2Ta_2O_9$ sintered at 1050°C for 2 h.

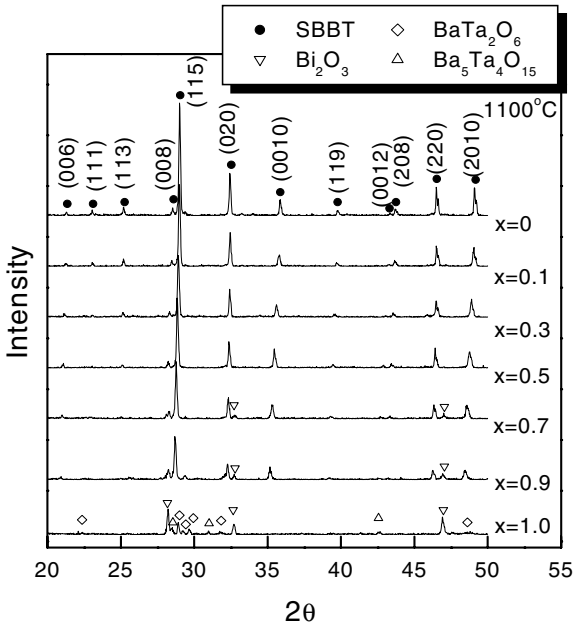

Figure 6 X-ray diffraction patterns of $(Sr_{1-x}Ba_x)Bi_2Ta_2O_9$ sintered at 1100°C for 2 h.

The diffraction patterns in Figs 4–6 also reveal that the ratios of the diffraction intensities $I_{(0010)}/I_{(020)}$depend on the sintering temperatures and doping amounts of barium ions. The above ratios indicate the c-axis preferred orientation of the layered perovskite. The c-axis preferred orientation of the specimens is defined as the following equation [22]:

$$F = (P - P_0)/(1 - P_0) \tag{1}$$

where $P = \sum I_{SBBT(00l)} / \sum I_{SBBT(hkl)}$, $I_{SBT(00l)}$ and $I_{SBT(hkl)}$ are the sum of intensities of (00l) and (hkl) reflections of the sintered $(Sr_{1-x}Ba_x)Bi_2Ta_2O_9$, and P_0 is the value of P for random orientated powders. Consequently, the value of F is zero when the powder is of random orientation, and it equals one if the powder is completely c-axis oriented. The F factors of the

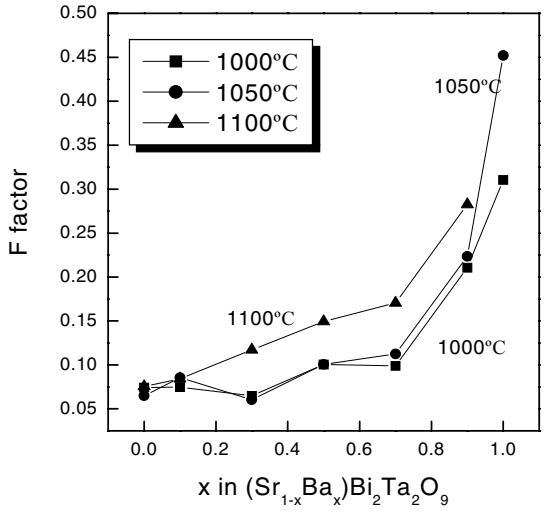

Figure 7 C-axis preferred orientation (F factor) of $(Sr_{1-x}Ba_x)Bi_2Ta_2O_9$ sintered at 1000, 1050, 1100°C for 2 h.

specimens sintered at 1000, 1050 and 1100°C are plotted in Fig. 7 as a function of the content of barium ions. The value of F monotonously increases with temperature. Furthermore, with more barium ions doped in $SrBi_2Ta_2O_9$, the degree of c-axis preferred orientation is significantly enhanced. The reasons for the variation in the degree of c-axis preferred orientation will be discussed in Section 3.3.

3.3. Microstructures of sintered $(Sr_{1-x}Ba_x)Bi_2Ta_2O_9$

The results described in previous sections reveal that barium ions have significant impact on the sintering density and c-axis preferred orientation. For elucidating the reasons underlying these changes, the microstructures of the surfaces of the sintered specimens were examined. The microstructures of 1050°C-sintered specimens are shown in Fig. 9. At $x = 0.1$, a considerably porous microstructure is observed (Fig. 8a), indicating the insufficient sinterability of the specimen with a low content of barium ions. The shape of the grains is nearly equal-axial and their grain size is around 0.5 μm. With an increase in the doping amounts of barium ions, the microstructure of the specimens markedly varies. In Fig. 8b, where $x = 0.7$, the microstructure of the specimen is well densified, revealing the high density of this specimen. In addition, the morphology of the grains turns into a plate-like shape with a size of 1.8–2.3 μm in length and 0.3–0.4 μm in thickness. When the value of x increases to 0.9 (Fig. 8c), the plate-like shape of the grains further develops and the size of these plates enlarges to 2–2.9 μm. This indicates that the doping of barium ions in $SrBi_2Ta_2O_9$ substantially results in not only the densification but also the anisotropic growth of grains. It has been reported that the grains of layered-perovskite materials are prone to grow along a-b planes and form a plate-like morphology during the sintering process at elevated temperatures [23, 24]. Once the plate-like grains are formed (Fig. 8b and c), they tend to lie on the surface of the specimens, rendering the basal a-b planes of grains to be arranged

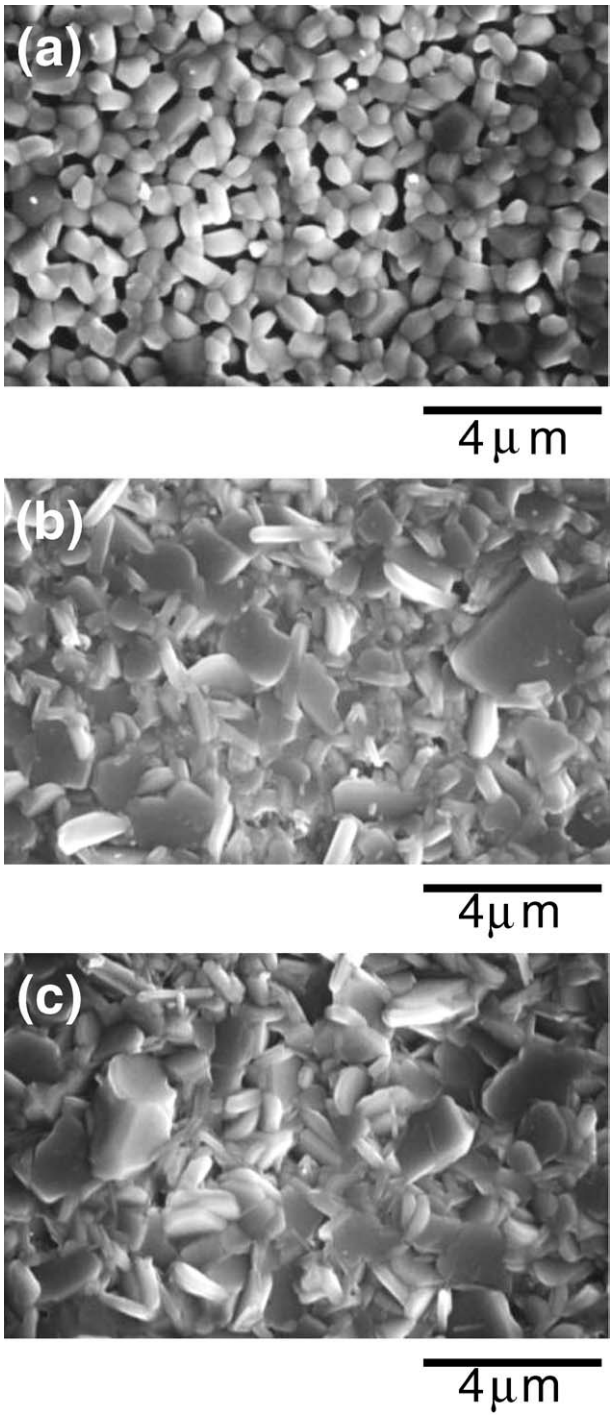

Figure 8 Microstructures of 1050°C-sintered $(Sr_{1-x}Ba_x)Bi_2Ta_2O_9$ for (a) $x = 0.1$, (b) $x = 0.7$, and (c) $x = 0.9$.

toward the specimen surfaces and a more stable stacking state was attained. As a result, the c-axis oriented grains are formed on the surfaces of barium ions-doped specimens. The doping of barium ions tends to facilitate the anisotropic growth of grains, and thus results in an increase in the degree of c-axis preferred orientation as shown in Fig. 7.

The microstructures of 1100°C-sintered specimens are shown in Fig. 9. At $x = 0.1$ (Fig. 9a), the microstructure of the specimens remains porous. At $x = 0.5$, a highly densified microstructure is produced (Fig. 9b), which is consistent with the sintering density shown in Fig. 3. On the other hand, when more barium ions are doped, the specimens decompose and different

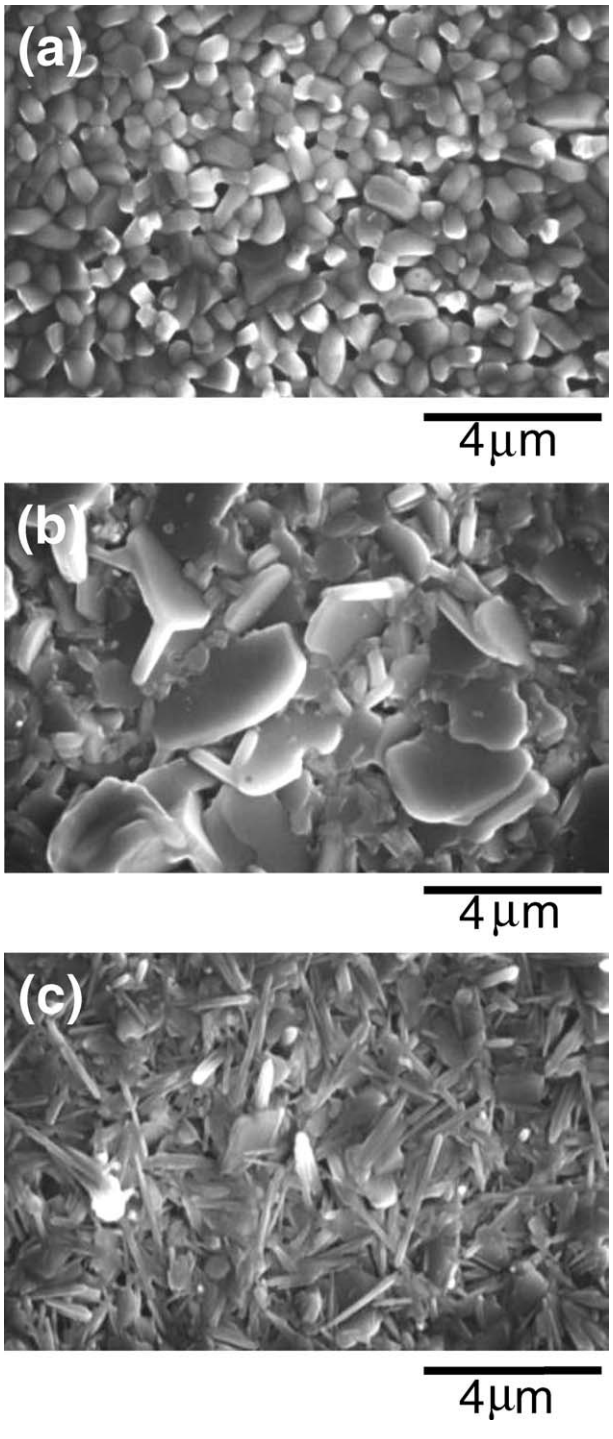

Figure 9 Microstructures of 1100°C-sintered $(Sr_{1-x}Ba_x)Bi_2Ta_2O_9$ for (a) $x = 0.1$, (b) $x = 0.5$, and (c) $x = 0.9$.

microstructures are formed. In Fig. 9c where $x = 0.9$, the plate-like grains disappear and large amounts of rod-like grains are produced instead. The width and length of these grains are around 0.15–0.2 and 1.8–2.2 μm, respectively. The thermal decomposition of barium-ion doped specimens is considered to lead to the formation of rod-like grains. The rod-like structure in the matrix results in the loose packing of the matrix that causes the expansion of the specimens, thereby making the density of the specimens to decrease as shown in Fig. 3. Consequently, for obtaining densified barium-ion doped $SrBi_2Ta_2O_9$ ceramics, it is necessary to precisely control the doping contents of barium ions and sintering temperatures.

4. Conclusions

The preparation and microstructures of $(Sr_{1-x}Ba_x)Bi_2Ta_2O_9$ layered perovskites have been investigated in this study. The lattice constants of the formed solid solutions increase with the doping amounts of barium ions. When $(Sr_{1-x}Ba_x)Bi_2Ta_2O_9$ powders are sintered, the relative densities rise with increasing the amounts of barium ions doped. Raising the sintering temperature to 1100°C causes the specimens to thermally decompose and thereby reduces the sintering density of $(Sr_{1-x}Ba_x)Bi_2Ta_2O_9$. The addition of barium ions in $SrBi_2Ta_2O_9$ increases not only the sintering density of the specimens but also the degree of *c*-axis preferred orientation. The occurrence of the *c*-axis preferred orientation is related to the anisotropic growth of the layer-structured grains. The doping of barium ions significantly varies the morphology and forms plate-like grains. When excess barium ions are doped, the specimens thermally decompose to produce rod-like grains, thereby causing a reduction in the density. The doping of barium ions plays an important role in influencing the sintering behavior, thermal stability, and microstructures of the $(Sr_{1-x}Ba_x)Bi_2Ta_2O_9$ solid solutions.

References

1. B. AURIVILLIUS, *Arkiv for Kemi* **1** (1949) 463.
2. *Idem.*, *ibid.* **2** (1950) 519.
3. E. C. SUBBARAO, *J. Amer. Ceram. Soc.* **45** (1962) 166.
4. K. AMANUMA, T. HASE and Y. MIYASAKA, *Appl. Phys. Lett.* **66** (1995) 221.
5. C. A. PAZ ARAUJO, J. D. CUCHIARO, M. C. SCOTT and L. D. MCMILLAN, *Nature* **374** (1995) 627.
6. P. C. JOSHI, S. O. RYU, X. ZHANG and S. B. DESU, *Appl. Phys. Lett.* **70** (1997) 1080.
7. C. H. LU and J. T. LEE, *Ceram. Inter.* **24** (1998) 285.
8. C. H. LU and Y. C. CHEN, *J. Eur. Ceram. Soc.* **19** (1999) 2909.
9. C. H. LU and C. Y. WEN, *J. Appl. Phys.* **86** (1999) 6335.
10. C. H. LU and Y. C. CHEN, *Integr. Ferro.* **31** (2000) 129.
11. M. A. ZURBUCHEN, G. ASAYAMA and D. G. SCHLOM, *Phys. Rev. Lett.* **88** (2002) 10760.
12. C. H. LU and C. H. WU, *J. Eur. Ceram. Soc.* **22** (2002) 707.
13. S. S. PARK, C. H. YANG, S. G. YONG, J. H. AHN and H. G. KIM, *J. Electronchem. Soc.* **144** (1997) 2855.
14. Y. ZHU, S. B. DESU, T. LI and S. RAMANATHAN, *J. Mater. Res.* **12** (1997) 783.
15. Y. C. CHEN and C. H. LU, *Integr. Ferro.* **31** (2000) 87.
16. C. H. LU and B. K. FANG, *J. Mater. Res.* **12** (1997) 2104.
17. S. B. DESU and D. P. VIJAY, *Mater. Sci. Eng. B* **32** (1995) 83.
18. C. H. LU and C. Y. WEN, *J. Eur. Ceram. Soc.* **20** (2000) 739.
19. T. SATO, K. SUGAHARA, T. KIJIMA and H. ISHIWARA, *Integr. Ferroelectr.* **39** (2001) 1119.
20. D. BHATTACHARYA, R. K. SINGH and P. H. HOLLOWAY, *J. Appl. Phys.* **70** (1991) 5433.
21. M. DECAMPS, D. REMIENS, L. CHABAL, B. JABER and B. THIERRY, *Appl. Phys. Lett.* **66** (1995) 685.
22. F. K. LOTGERING, *J. Inorg. Nucl. Chem.* **9** (1959) 113.
23. S. H. LIN, S. L. SWAETZ, W. A. SCHULZE and J. V. BIGGERS, *J. Amer. Ceram. Soc.* **66** (1983) 881.
24. H. WATANABE, T. KIMURA and T. YAMAGUCHI, *ibid.* **74** (1991) 139.

Received 22 May 2003
and accepted 15 January 2004